Temperature dependence of ultrafast phonon dynamics in graphite

M. Scheuch, T. Kampfrath, M. Wolf, K. von Volkmann, C. Frischkorn, and L. Perfetti

Citation: Applied Physics Letters **99**, 211908 (2011); doi: 10.1063/1.3663867
View online: http://dx.doi.org/10.1063/1.3663867
View Table of Contents: http://scitation.aip.org/content/aip/journal/apl/99/21?ver=pdfcov
Published by the AIP Publishing

Temperature dependence of ultrafast phonon dynamics in graphite

M. Scheuch,[1,2,a)] T. Kampfrath,[1,2] M. Wolf,[1,2] K. von Volkmann,[2,3] C. Frischkorn,[1,2] and L. Perfetti[2,4]
[1]*Fritz-Haber-Institut der Max-Planck-Gesellschaft, Berlin, Germany*
[2]*Fachbereich Physik, Freie Universität Berlin, Berlin, Germany*
[3]*APE Angewandte Physik und Elektronik GmbH, Berlin, Germany*
[4]*Laboratoire des Solides Irradiés, Ecole polytechnique, Palaiseau cedex, France*

(Received 17 October 2011; accepted 25 October 2011; published online 22 November 2011)

Nonequilibrium optical phonons are generated in graphite following the excitation of electron-hole pairs with a femtosecond laser pulse. Their energy relaxation is probed by means of terahertz pulses. We find that the hot-phonon lifetime increases by a factor of 2 when the sample temperature decreases from 300 to 5 K. These results suggest that the energy relaxation in graphite at room temperature and above is dominated by the anharmonic decay of hot A_1' phonons at the K point into acoustic phonons with energies of about 10 meV. © *2011 American Institute of Physics*. [doi:10.1063/1.3663867]

In recent years, graphene and graphite have earned great interest due to their ability to sustain high current densities.[1–4] For this reason, carbon-based materials are considered as promising alternatives to silicon for the development of nanoelectronic devices. Transport experiments in graphite and carbon nanotubes have revealed a critical driving electric field at which a crossover from ballistic to diffusive transport occurs. This crossover was assigned to the scattering of high-energy electrons with a minor subset of strongly coupled optical phonons (SCOPs), which acquire a higher effective temperature than the remaining, still cold phonons.[5] Density functional theory (DFT) calculations of electron-phonon coupling have identified the SCOPs in graphite as the modes with the highest energies (≈0.2 eV) at the Γ point (E_{2g}) and the K point (A_1') of the Brillouin zone.[6,7]

Hot SCOPs can also be generated by illuminating graphite with a femtosecond laser pulse.[8–20] The photoexcited electrons thermalize and concurrently transfer most of their excess energy to the small phonon subset of SCOPs within 0.5 ps.[9–16,21] A quasi-equilibrium between electrons and SCOPs is established. The hot phonons cool on a picosecond timescale by energy transfer to the other, cold phonons. Up to now, however, the pathway of the hot-phonon relaxation has not yet been studied in detail. Theory work predicts that the SCOP cooling proceeds via anharmonic decay, which becomes significantly faster with increasing ambient temperature.[22] Such behavior has already been indicated by time-resolved Raman spectroscopy at temperatures from 300 to 700 K.[13] In order to elucidate the role of decay channels involving low-energy phonons, experiments have to be performed at lower temperatures as well.

In this letter, we make use of time-resolved THz spectroscopy to measure the energy decay rate of the hot-phonon system in photoexcited, highly ordered pyrolytic graphite (HOPG) as a function of temperature from 5 to 300 K. Due to its low photon energy, THz radiation is particularly sensitive to the distribution of charge carriers in the vicinity of the Fermi energy.[23] We observe a pronounced increase of the SCOP lifetime with decreasing temperature. This result is consistent with a dominant SCOP decay into acoustic modes with energies of only 10 meV via anharmonic coupling.

We apply 12-fs laser pulses with 780-nm center wavelength from an 80-MHz Ti:sapphire oscillator to generate THz pulses via difference frequency mixing in a GaSe crystal.[24] The resulting THz pulses cover a range from 10 to 30 THz with a duration of 100 fs. The detection of the THz electric field via electro-optic sampling in ZnTe allows us to simultaneously measure both amplitude and phase of the THz transient.[25] Part of the oscillator output is used to excite the sample prior to THz probing at variable delay times τ. The samples are prepared by peeling off flakes from a HOPG crystal, resulting in a 20-nm thin film supported on a diamond substrate which is mounted in a cryostat that can be cooled down to 5 K. Transmitting under normal incidence, the THz pulse probes the optical properties perpendicular to the c axis. In our setup, we measure the electric fields $E_0(t)$ and $E_0(t) + \Delta E_\tau(t)$ of a THz pulse that has traversed an unexcited and excited sample, respectively. Here, t denotes the time axis of the THz transient.

Figure 1(a) shows the pump-induced changes $\Delta E_\tau(t)$ in the transmitted THz field along with the reference field $E_0(t)$. In order to monitor the relaxation of the excited sample, we

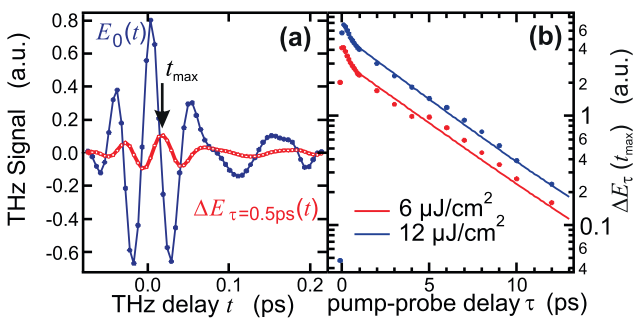

FIG. 1. (Color online) (a) THz waveform $E_0(t)$ after transmission through unexcited graphite and pump-induced changes $\Delta E_\tau(t)$ at $\tau = 0.5$ ps. Arrow: pump-induced signal maximum $\Delta E_\tau(t_{max})$. (b) $\Delta E_\tau(t_{max})$ as function of pump-probe delay at 300 K at various pump fluences. Solid lines: biexponential fit.

a)Author to whom correspondence should be addressed: Electronic mail: scheuch@fhi-berlin.mpg.de.

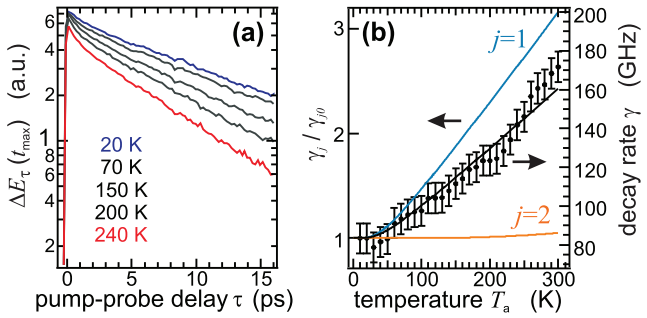

FIG. 2. (Color online) (a) Decay of $\Delta E_\tau(t_{max})$ vs. τ at several temperatures. (b) T_a dependence of the resulting scattering rates γ (right axis). Solid lines: normalized contributions (left axis) of phonon decay channels $j = 1, 2$ shown in Fig. 3(b) and fit of $\gamma_1 + \gamma_2$ to the experimentally determined γ.

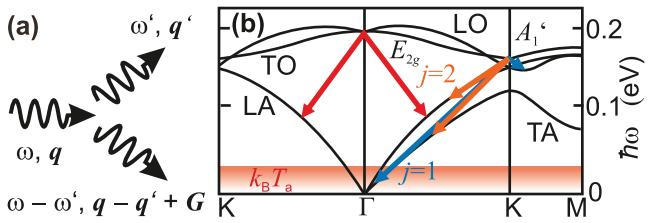

FIG. 3. (Color online) (a) Schematic of phonon decay into two phonons. Wavevector q and energy $\hbar\omega$ conservation restricts the set of allowed decay channels. G is a reciprocal lattice vector. (b) Schematic of graphite phonon dispersion. Arrows: examples of allowed decay channels of SCOPs according to Ref. 6. Shaded area indicates the thermal energy $k_B T_a$ with $T_a \leq 300$ K.

set $t = t_{max}$, where the maximum of the pump-induced THz transient is located. The resulting trace of $\Delta E_\tau(t_{max})$ vs. pump-probe delay τ is shown in Fig. 1(b) for two pump fluences. All traces exhibit a biexponential decay with a fast and slow component featuring time constants of 0.8 ps and 5.5 ps at 300 K, respectively. As indicated by the identical slopes of the curves in Fig. 1(b), the slow time constants are found to be independent of the applied laser fluence demonstrating that they represent sample-intrinsic quantities.

Qualitatively similar two-component dynamics have been observed using other time-resolved techniques.[8,11–18] Further analysis[9–12] and simulations based on Boltzmann Peierls rate equations[21] have shown that the faster signal component reflects the thermalization of the electronic subsystem via electron-electron and electron-phonon scattering accompanied by energy transfer to the SCOPs. Since the Fermi surface of graphite consists of only two small pockets, the emitted phonons have a wavevector whose in-plane component is located close to the Γ or K point of the Brillouin zone.[9] Despite the small fraction of available phonon states, the remarkably fast electron cooling is brought about by the strong electron-phonon coupling in graphite.[6,7] After less than 0.5 ps, the SCOPs have absorbed more than 90% of the electronic excess energy, and a quasi-equilibrium of electrons and SCOPs is established.[9–12] The slower component of the pump-probe signal is associated with the cooling of the combined subsystem electrons plus hot SCOPs.[9,10] Since most of the pump energy is contained in the hot phonons, the slow decay directly reflects the SCOP lifetime.[10,21]

In order to obtain deeper insights into the energy decay of the SCOPs, we took pump-probe traces $\Delta E_\tau(t_{max})$ at various ambient temperatures T_a. As shown in Fig. 2(a), the decay of the slower component becomes faster with rising T_a. We obtain the hot SCOP lifetimes as the time constant $1/\gamma$ of the slower relaxation component of the signal. Fig. 2(b) shows the resulting decay rate γ vs. T_a. Note that γ increases by more than 100% when the ambient temperature increases from 5 to 300 K.

The cooling of the electron-SCOP system proceeds via annihilation of an electron-hole pair[26] or a SCOP,[22] both resulting in phonon emission into cold lattice modes. The first scenario is not expected to occur on the picosecond time scale observed in our experiment as it involves emitted phonons with energies more than one order of magnitude smaller than those of the SCOPs.[10] In addition, the coupling of these phonons to the electrons is negligible as compared to the SCOPs.[6] Finally, according to the two-temperature model,[26] the first mechanism should result in a slower decay with increasing T_a, contrary to our findings [Fig. 2(b)]. Thus, it is reasonable to assume the combined cooling of electrons and hot SCOPs mediated by anharmonic phonon-phonon coupling which induces the decay of a SCOP into two phonons with lower energy[10,13,22] [Fig. 3(a)]. Each decay channel j contributes

$$\gamma_j = \gamma_{j0}[1 + b(\omega'_j, T_a) + b(\omega_j - \omega'_j, T_a)] \quad (1)$$

to the total energy decay rate $\gamma = \sum \gamma_j$ of the hot-phonon system.[27] Here, γ_{j0} is the rate at vanishing sample temperature, b the Bose-Einstein distribution, ω_j the SCOP frequency, and ω'_j and $\omega_j - \omega'_j$ are the frequencies of the emitted phonons. Each of these three-phonon processes has to conserve phonon energy and wavevector, thus greatly reducing the set of allowed final modes. Using the phonon dispersion relation of graphite, an experimentally determined function,[7] it has been found[22] that the lower phonon energy $\hbar\omega'_j$ can only derive from a few narrow intervals between 0 and $\hbar\omega_j/2$. Examples of decay events are shown in Fig. 3(b).

The interval with the lowest phonon energies is centered around $\hbar\omega'_j = 10.5$ meV and associated with acoustic phonons emitted in the decay of the $A'_1 - K$ mode[22] [blue arrows in Fig. 3(b)]. Using Eq. (1), we calculate the normalized rate γ_1/γ_{10} of this decay channel as a function of T_a. As seen from Fig. 2(b), γ_1 increases by more than a factor of 2 when the temperature increases from 5 to 300 K. This strong temperature sensitivity arises, because the phonon energy $\hbar\omega'$ is comparable to the thermal energy $k_B T_a$ [shaded area in Fig. 3(b)]. In contrast, considering an allowed decay channel with the next-higher energy $\hbar\omega'_2 = 60$ meV of the emitted low-energy phonon[22] [orange arrows in Fig. 3(b)], we obtain a curve with nearly negligible temperature dependence [$j = 2$ curve in Fig. 2(b)]. Similar curves are obtained for all remaining decay channels j as they involve even higher energies $\hbar\omega'_j$. An example is the symmetric decay of the E_{2g}-Γ mode [red arrows in Fig. 3(b)]. Therefore, it is sufficient to fit a linear combination of γ_1 and γ_2 to the measured decay curve of γ vs. T_a, with γ_{10} and γ_{20} as fit parameters. Whereas γ_2 merely contributes a constant offset, γ_1 sets the slope of the curve. Best fit results are obtained for $1/\gamma_{10} = 22.1$ ps and $1/\gamma_{20} = 30.5$ ps [Fig. 2(b)]. Thus, our results are compatible with the notion that the energy relaxation of the hot SCOPs

is dominated by the decay of A_1' phonons at the K point into acoustic phonons with energies of about 10 meV.

Previous temperature-dependent studies of the SCOP decay of photoexcited graphite made use of time-resolved incoherent Raman scattering and report decay times of 2.2 ps (Ref. 13) and 2.4 ps (Ref. 17) at 300 K, considerably shorter than the 5.5 ps observed here. It should be noted that studies based on other time-resolved techniques such as transient reflectance or transmittance,[8,18] photoelectron spectroscopy,[12] and electron diffraction[16] also report a broad variety of time constants of the slow signal component. This variety may be related to the use of different probing techniques and samples of different thickness.[18,20] Especially, since both THz (Ref. 9) and Raman signal[10] reflect the hot-phonon temperature, the different time constants measured most likely arise from the samples used. In this work, the graphite thin film is homogeneously excited, whereas transport effects into the inhomogeneously excited bulk crystal used by Ref. 13 may accelerate the dynamics inside the probed volume. However, despite the different time constants, the relative changes as a function of T_a are comparable for the Raman-based and our work: an increase of the phonon decay rate by about 70% was observed by increasing T_a from 300 to 700 K (Refs. 13 and 17), while a 100% increase from 5 to 300 K is found in our experiment. We also note that our fit to the measured $\gamma(T_a)/\gamma(300\,\mathrm{K})$ would also give a reasonable description of the normalized time-resolved Raman data. Conversely, the model of Ref. 13 would not yield a good description of our data as it involves too high phonon energies $\hbar\omega'$. In other words, low-temperature experiments allow a better identification of the phonon decay processes involving small phonon energies of the order of 10 meV.

We finally compare our results to DFT calculations[22,28] of the lifetime of various phonon modes at the Γ and K points. Our results agree well with the predicted temperature dependence of the $A_1' - \mathrm{K}$ lifetime [see Fig. 4(a) in Ref. 22] as well as the branching ratio of the different decay processes j; we have $\gamma_{01}/\sum\gamma_{0j} = 0.58$ as inferred from our experiment and 0.56 from theory. Absolute numbers agree roughly: $1/\gamma_{10} = 22.1$ ps, as derived from experiment, is larger than $1/\gamma_{10} = 8.2\ \mathrm{ps}/0.56 = 14.6$ ps predicted by theory. However, theory[22] also suggests a strong contribution from the decay of the $E_{2g^-}\Gamma$ mode, with a much shorter lifetime of about 3.3 ps at vanishing temperature. Such short phonon lifetimes are not observed in our experiment. The reason for this discrepancy is not yet understood.

In conclusion, we have observed a pronounced acceleration of the hot-phonon decay in graphite in the temperature range when temperature is increased from 5 to 300 K. Our results suggest that this relaxation proceeds via anharmonic decay of hot SCOPs into acoustic phonons with low energy. As a consequence, the hot-phonon population observed in high-field transport in graphite and graphene[4] should roughly scale with the inverse of the ambient temperature. This notion would imply an increased resistance and a lower breakdown threshold for cooled graphite-based devices.

The authors would like to thank the German Research Foundation DFG for financial support via Sfb 450.

[1]K. S. Novoselov, A. K. Geim, S. V. Morozov, D. Jiang, Y. Zhang, S. V. Dubonos, I. V. Grigorieva, and A. A. Firsov, Science **306**, 666 (2004).
[2]J. Moser, A. Barreiro, and A. Bachtold, Appl. Phys. Lett. **91**, 163513 (2007).
[3]A. Barreiro, M. Lazzeri, J. Moser, F. Mauri, and A. Bachtold, Phys. Rev. Lett. **103**, 076601 (2009).
[4]S. Berciaud, M. Y. Han, K. F. Mak, L. E. Brus, P. Kim, and T. F. Heinz, Phys. Rev. Lett. **104**, 227401 (2010).
[5]A. Javey, J. Guo, M. Paulsson, Q. Wang, D. Mann, M. Lundstrom, and H. Dai, Phys. Rev. Lett. **92**, 106804 (2004).
[6]S. Piscanec, M. Lazzeri, F. Mauri, A. C. Ferrari, and J. Robertson, Phys. Rev. Lett. **93**, 185503 (2004).
[7]J. Maultzsch, S. Reich, C. Thomsen, H. Requardt, and P. Ordejón, Phys. Rev. Lett. **92**, 075501 (2004).
[8]H. Wang, J. H. Strait, P. A. George, S. Shivaraman, V. B. Shields, M. Chandrashekhar, J. Hwang, F. Rana, M. G. Spencer, C. S. Ruiz-Vargas, and J. Park, Appl. Phys. Lett. **96**, 081917 (2010).
[9]T. Kampfrath, L. Perfetti, F. Schapper, C. Frischkorn, and M. Wolf, Phys. Rev. Lett. **95**, 187403 (2005).
[10]H. Yan, D. Song, K. F. Mak, I. Chatzakis, J. Maultzsch, and T. F. Heinz, Phys. Rev. B **80**, 121403(R) (2009).
[11]M. Breusing, C. Ropers, and T. Elsaesser, Phys. Rev. Lett. **102**, 086809 (2009).
[12]Y. Ishida, T. Togashi, K. Yamamoto, M. Tanaka, T. Taniuchi, T. Kiss, M. Nakajima, T. Suemoto, and S. Shin, Sci. Rep. **1**, 64 (2011).
[13]I. Chatzakis, H. Yan, D. Song, S. Berciaud, and T. F. Heinz, Phys. Rev. B **83**, 205411 (2011).
[14]G. Moos, C. Gahl, R. Fasel, M. Wolf, and T. Hertel, Phys. Rev. Lett. **87**, 267402 (2001).
[15]K. Ishioka, M. Hase, M. Kitajima, L. Wirtz, A. Rubio, and H. Petek, Phys. Rev. B **77**, 121402(R) (2008).
[16]S. Schäfer, W. Liang, and A. H. Zewail, New J. Phys. **13**, 063030 (2011).
[17]K. Kang, D. Abdula, D. G. Cahill, and M. Shim, Phys. Rev. B **81**, 165405 (2010).
[18]R. W. Newson, J. Dean, B. Schmidt, and H. M. van Driel, Opt. Express **17**(4), 2326 (2009).
[19]H. Choi, F. Borondics, D. A. Siegel, S. Y. Zhou, M. C. Martin, A. Lanzara, and R. A. Kaindl, Appl. Phys. Lett. **94**, 172102 (2009).
[20]P. J. Hale, S. M. Hornett, J. Moger, D. W. Horsell, and E. Hendry, Phys. Rev. B **83**, 121404(R) (2011).
[21]S. Butscher, F. Milde, M. Hirtschulz, E. Malic, and A. Knorr, Appl. Phys. Lett. **91**, 203103 (2007).
[22]N. Bonini, M. Lazzeri, N. Marzani, and F. Mauri, Phys. Rev. Lett. **99**, 176802 (2007).
[23]R. Ulbricht, E. Hendry, J. Shan, T. F. Heinz, and M. Bonn, Rev. Mod. Phys. **83**, 543 (2011).
[24]R. Huber, A. Brodschelm, F. Tauser, and R. Leitenstorfer, Appl. Phys. Lett. **76**, 3191 (2000).
[25]T. Kampfrath, J. Nötzold, and M. Wolf, Appl. Phys. Lett. **90**, 231113 (2007).
[26]P. B. Allen, Phys. Rev. Lett. **59**, 1460 (1987).
[27]A. Laubereau, D. von der Linde, and W. Kaiser, Phys. Rev. Lett. **27**, 802 (1971).
[28]N. Bonini, R. Rao, A. M. Rao, M. Marzari, and J. Menéndez, Phys. Status Solidi B **245**(10), 2149 (2008).